# Distinct functions of the *Drosophila* Nup153 and Nup214 FG domains in nuclear protein transport

Nafiseh Sabri, Peggy Roth, Nikos Xylourgidis, Fatemeh Sadeghifar, Jeremy Adler, and Christos Samakovlis

Department of Developmental Biology, Wenner-Gren Institute, Stockholm University, S-10691 Stockholm, Sweden

The phenylanine-glycine (FG)–rich regions of several nucleoporins both bind to nuclear transport receptors and collectively provide a diffusion barrier to the nuclear pores. However, the in vivo roles of FG nucleoporins in transport remain unclear. We have inactivated 30 putative nucleoporins in cultured *Drosophila melanogaster* S2 cells by RNA interference and analyzed the phenotypes on importin α/β–mediated import and CRM1-dependent protein export. The fly homologues of FG nucleoporins Nup358, Nup153, and Nup54 are selectively required for import. The FG repeats of Nup153 are necessary for its function in transport, whereas the remainder of the protein maintains pore integrity. Inactivation of the CRM1 cofactor RanBP3 decreased the nuclear accumulation of CRM1 and protein export. We report a surprisingly antagonistic relationship between RanBP3 and the Nup214 FG region in determining CRM1 localization and its function in protein export. Our data suggest that peripheral metazoan FG nucleoporins have distinct functions in nuclear protein transport events.

## Introduction

Yeast and vertebrate nuclear pore complexes (NPCs) are structurally similar and consist of multiple copies of ∼30 different nucleoporins (Rout et al., 2000; Cronshaw et al., 2002). Approximately one third of all nucleoporins (Nups) carry phenylanine-glycine (FG) repeats of variable length. They are found at the nuclear basket, cytoplasmic fibers, and the central part of the NPC and can bind to both importins and exportins (Tran and Wente, 2006). X-ray crystallography has mapped the contact sites between FG repeats and importin β, and mutations altering these amino acids in importin β also reduce nuclear protein import (Bayliss et al., 2002). The extended conformation of the FG regions, their abundance in the NPC, and their differential affinity for transport receptors suggest that they are major determinants of transport through the channel. However, genetic and biochemical experiments in yeast show that half of the FG repeats can be removed without any defect in protein transport and cell viability (Strawn et al., 2004).

The FG domain nucleoporins collectively provide a diffusion barrier to the pore. According to the virtual gating model, macromolecules are excluded from the pore by the fluctuations of unfolded peripheral FG domains. The local interaction between transport receptors and peripheral FG repeats traps the cargo, increases its residence time, and facilitates passage through the pore (Rout et al., 2003). In the selective phase partitioning model, intermolecular hydrophobic interactions between the FG repeats create a selective permeability barrier that prohibits free diffusion through the NPC. The interaction of nuclear transport receptors with distinct FG nucleoporins locally breaks the mesh and allows passage through the NPC (Frey et al., 2006). Are the mechanistic functions of all FG nucleoporins the same? Do individual metazoan FG nucleoporins contribute to protein transport differently than their yeast counterparts? We addressed these questions by functional analysis of the NPC using inducible GFP transport reporters in conjunction with RNAi in *Drosophila melanogaster* S2 cells.

Correspondence to Christos Samakovlis: christos@devbio.su.se

Abbreviations used in this paper: cNLS, classic NLS; dsRNA, double-stranded RNA; FG, phenylanine-glycine; NES, nuclear export signal; NPC, nuclear pore complex.

The online version of this article contains supplemental material.

## Results and discussion

### An RNAi screen for nucleoporin function in protein transport

We established inducible S2 cells expressing GFP, GFP fused to a classic NLS (cNLS [cNLS-GFP]), or GFP carrying a nuclear export signal (NES [GFP-NES]). Living cells expressing native GFP showed a homogenous distribution of the fluorescent signal (Fig. 1 A). The cNLS-GFP reporter accumulated in nuclei, whereas the GFP-NES cargo was localized predominantly in the cytoplasm (Fig. 1 A).

We tested whether the cNLS-GFP and GFP-NES reporters are cargoes of importin α/βs and CRM1. We first treated


The Journal of Cell Biology, Vol. 178, No. 4, August 13, 2007 557–565
http://www.jcb.org/cgi/doi/10.1083/jcb.200612135

the cell lines with double-stranded RNA (dsRNA) against the *Drosophila* homologues of importin α1, α2 (pendulin), α3, β (ketel), or kapβ3 (Malik et al., 1997; Lippai et al., 2000). Only the addition of importin α3 and β dsRNAs reduced the relative levels of nuclear cNLS-GFP. The distribution of the GFP and GFP-NES reporters was unaffected by the dsRNA treatments (Fig. S1 A, available at http://www.jcb.org/cgi/content/full/jcb.200612135/DC1; and not depicted). Thus, the cNLS-GFP reporter is transported into the nucleus by importin α3/β. In parallel, we treated the reporter cell lines with dsRNA for CRM1 (*emb*; Collier et al., 2000). The nuclear intensity of GFP-NES was increased in CRM1-depleted cells. This phenotype was comparable with the one generated by the treatment of GFP-NES cells with leptomycin, a CRM1-specific inhibitor (Fig. S1 B). Therefore, the cytoplasmic accumulation of GFP-NES provides a functional assay for CRM1-mediated export.

To assess the relative contributions of the NPC components on cNLS import and NES export, we searched the *Drosophila* genome database for nucleoporins. We identified a set of 30 putative nucleoporins and a protein export cofactor, RanBP3, in *Drosophila* (Table S1, available at http://www.jcb.org/cgi/content/full/jcb.200612135/DC1). We did not detect any Pom121 and Nup180 homologues in the fly genome. The putative nucleoporin function of the selected *Drosophila* genes was also predicted by the Inparanoid algorithm (O'Brien et al., 2005), which classified them as orthologues of human genes encoding nucleoporins (Table S1). For simplicity, we will refer to the putative *Drosophila* nucleoporins by the names of their human homologues.

We generated dsRNAs targeting each candidate nucleoporin and tested gene inactivation efficiency in the reporter cell lines by RT-PCR and by immunostainings and Western blots in cases in which specific antibodies were available (Fig. S1, C–E). The dsRNA treatments considerably reduced the endogenous gene product after 4 d and allowed functional analysis of the genes in protein transport. The cellular distribution of each GFP reporter was assessed in parallel 4 d (Table S1) and 6 d (unpublished data) after the addition of dsRNA to the cultures. To avoid artifacts as a result of the potential off-target effects of the dsRNAs, we generated a second set of dsRNAs for all nucleoporins that scored positive in the primary screen. These dsRNAs generated similar defects in the distribution of the reporters, arguing for phenotype specificity (see below and Fig. S2, A–C; available at http://www.jcb.org/cgi/content/full/jcb.200612135/DC1).

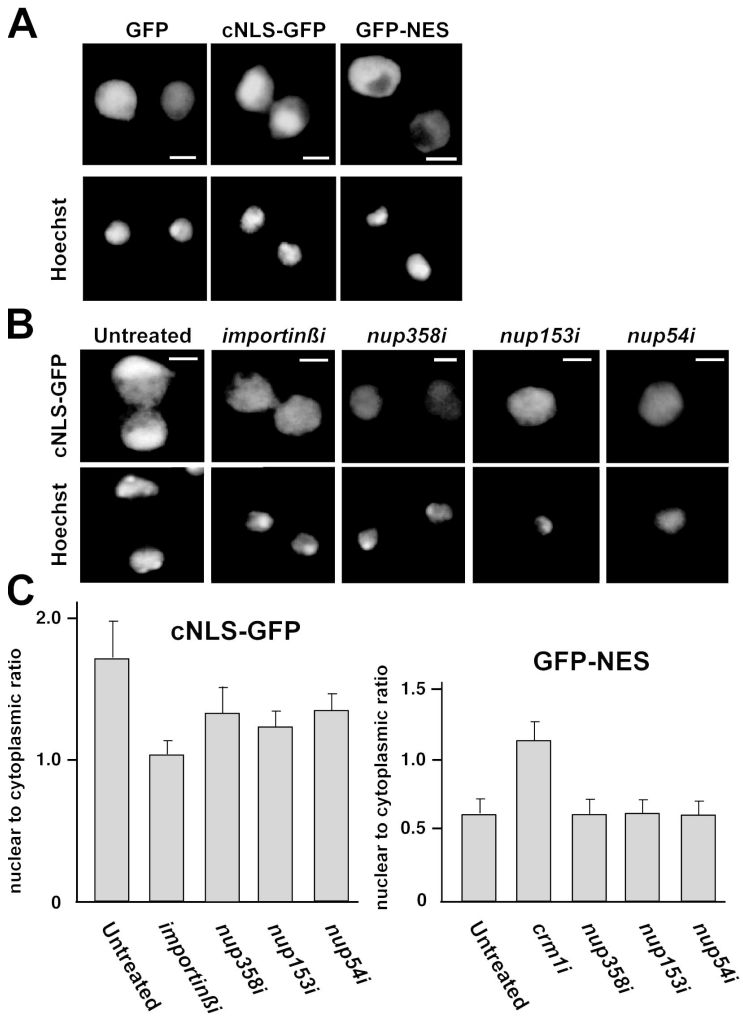


Figure 1. **cNLS-GFP import defects in Nup358, Nup153, and Nup54 RNAi cells.** (A) Localization of GFP, cNLS-GFP, and GFP-NES in S2 cells. Hoechst staining visualizes nuclei. (B) Cells expressing cNLS-GFP were treated with importin β, Nup358, Nup153, or Nup54 dsRNAs. (C) Ratios of nuclear to cytoplasmic cNLS-GFP (left) and GFP-NES (right) intensities in untreated and RNAi cells. dsRNA treatments reduced the nuclear accumulation of cNLS-GFP compared with untreated cells ($P < 0.0001$ by pair-wise *t* test). GFP-NES distribution was only affected in *crmi* cells ($P > 0.05$ by pair-wise *t* test for the nucleoporins). Error bars indicate SD. 30–35 cells were quantified for each treatment. Bars, 5 μm.

### Selective requirement of Nup358, Nup153, and Nup54 in cNLS-GFP import

Cells treated with dsRNAs for Nup358, Nup153, or Nup54 exhibited a clear reduction in cNLS-GFP nuclear concentration but showed no defects in GFP-NES and GFP localization, suggesting a selective role for Nup358, Nup153, and Nup54 in cNLS-protein import (Fig. 1, B and C; Fig. S2 D; and Table S1).

The import phenotype might be secondary to structural defects in the NPC caused by silencing of the nucleoporin genes. To assess NPC integrity, we stained dsRNA-treated cells with the nucleoporin marker mAb414 and a panel of specific antibodies against NPC components: Nup214 and Nup88 at the cytoplasmic face (Fornerod et al., 1997), gp210 at the central core (Wozniak and Blobel, 1992), and TPR in the nuclear basket (Cordes et al., 1997). We found a pronounced reduction in mAb414 and anti-TPR rim labeling in Nup153 dsRNA-treated cells (Fig. 2). In addition, a substantial amount of Nup214 and its binding partner Nup88 was displaced from the pore (Fig. 2). Thus, both the cytoplasmic and nuclear basket nucleoporins are severely affected in Nup153 RNAi cells. We did not detect any phenotype with the gp210 antibody, suggesting that this part of the central core was intact (Fig. 2). None of the NPC composition defects in Nup153-depleted cells were detected in cells lacking Nup358 or Nup54, arguing that the import deficiency in these cells was not caused by major changes in pore integrity.

We further examined whether the RNAi inactivations caused defects in the localization or the amount of importin β by in situ stainings and Western blots (Fig. 3, A and B). Untreated cells showed the characteristic rim-staining pattern of importin β. Nup358 RNAi cells exhibited a weak cytoplasmic staining. The importin β signal was also reduced in Nup54 dsRNA-treated cells, but its localization was not affected. In Nup153 RNAi cells, the levels of importin β were not appreciably affected, but a substantial fraction of the protein was displaced from the rim

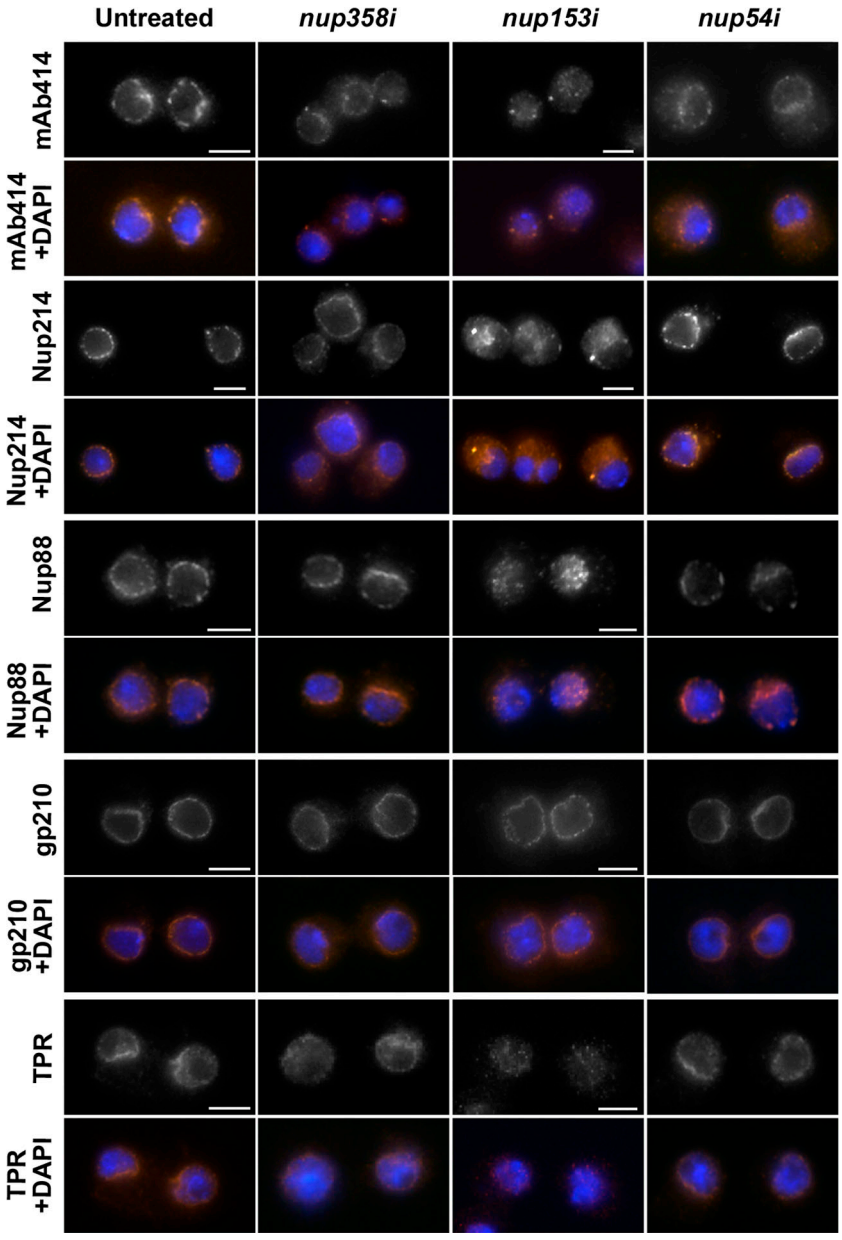


Figure 2. **Localization of nuclear pore components in cells defective in cNLS-GFP import.** Cells subjected to Nup358, Nup153, or Nup54 dsRNA treatment stained with mAb414 and antibodies against Nup214, Nup88, gp210, and TPR. DAPI staining visualizes nuclei. Bars, 5 μm.

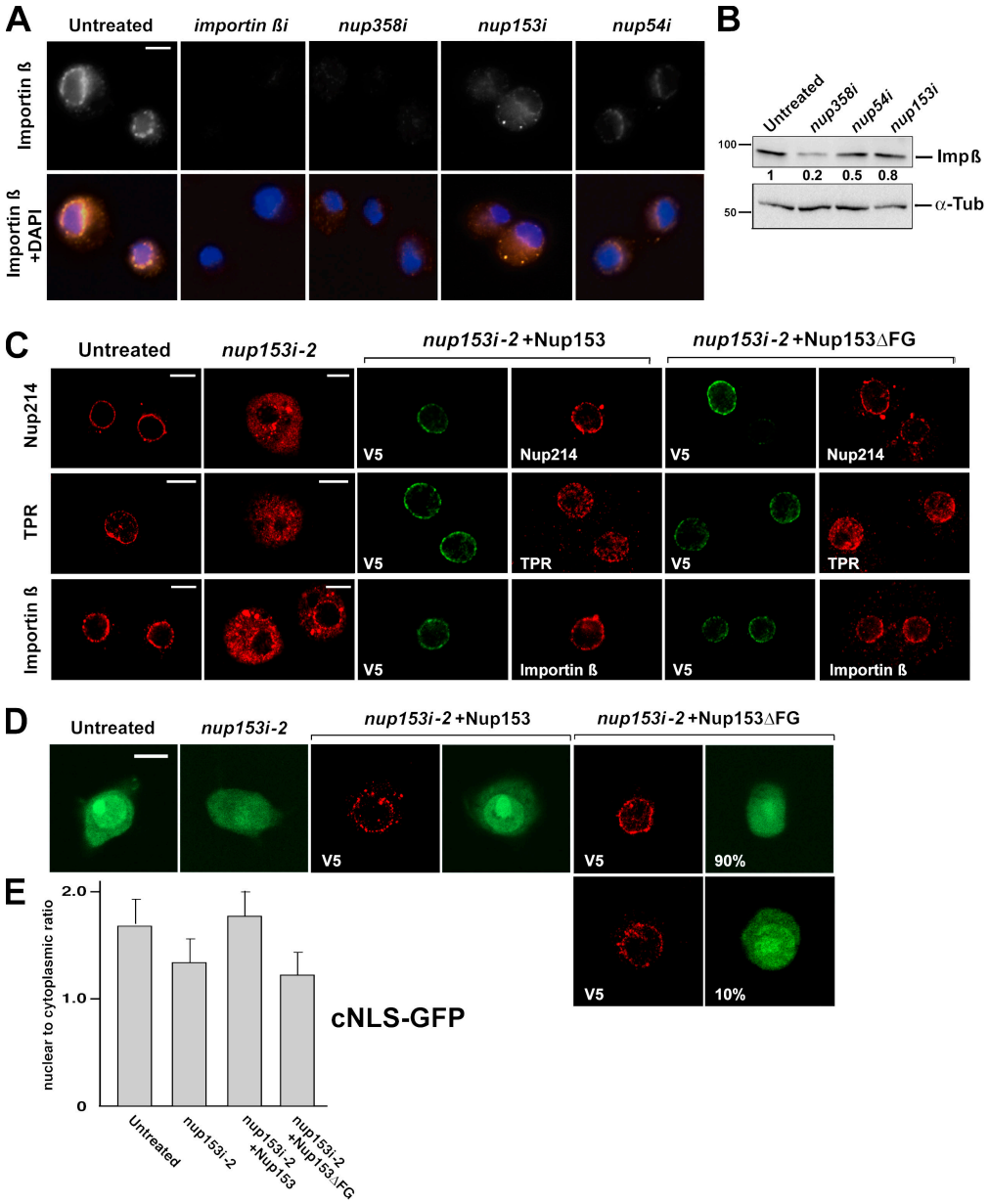


Figure 3. **Separable roles of Nup153 in pore integrity and cNLS import.** (A) Cells treated with importin β, Nup358, Nup153, or Nup54 dsRNAs stained for importin β. DAPI staining visualizes nuclei. (B) Western blot of extracts from Nup358, Nup54, and Nup153 RNAi cells probed with anti–importin β and antitubulin antibodies. Importin β intensities were normalized against tubulin. Numbers indicate the relative levels of importin β in each sample. (C) Function of full-length Nup153 and Nup153ΔFG in pore integrity and importin β localization. The first column shows untreated cells. The second column shows cells treated with dsRNA against the 3′ untranslated region of Nup153 (*nup153i-2*). The other columns show cells treated in parallel and transfected with either V5-Nup153 or V5-Nup153ΔFG plasmids. Cells were stained for V5, Nup214, TPR, and importin β. V5 staining visualizes the expression of Nup153 fusion proteins. All panels show confocal sections. (D) cNLS-GFP cells treated as in C stained for V5 (red). GFP flourescence is shown in green. cNLS-GFP distribution was restored in only 10% of cells expressing Nup153ΔFG. (E) Quantification of nuclear to cytoplasmic cNLS-GFP intensity ratios in Nup153 RNAi cells. The expression of V5-Nup153 ($P < 0.0001$ by pair-wise *t* test) but not of V5-Nup153ΔFG ($P > 0.05$ by pair-wise *t* test) restored cNLS-GFP distribution. Error bars indicate SD. 20–25 cells were quantified in each case. Bars (A), 5 μm; (C and D) 2.5 μm.

into the cytoplasm (Fig. 3, A and B). Thus, in all cases, the nuclear import deficit of the dsRNA-treated cells correlates with defects in the levels and/or localization of importin β. Neither the distribution nor the intensity of CRM1 staining was appreciably changed in these cells (Fig. S2 E), implying that Nup358, Nup153, and Nup54 are selectively required for importin β–mediated import. Our genetic analysis of Nup153 and Nup54 function in cNLS import is consistent with studies in yeast (Nup57; Bucci and Wente, 1998), *Xenopus laevis* oocytes (Nup153 [Walther et al., 2001] and Nup54 [Finlay et al., 1991]), and HeLa cells (Nup153; Shah and Forbes, 1998) using immunodepletion and overexpression experiments. However, the role of *Drosophila* Nup358 is surprising. Nup358 is the major component of the cytoplasmic filaments, and immunodepletion of its *Xenopus* homologue does not cause cNLS import defects in oocyte nuclei (Walther et al., 2002). *Drosophila* Nup358 is essential for importin β

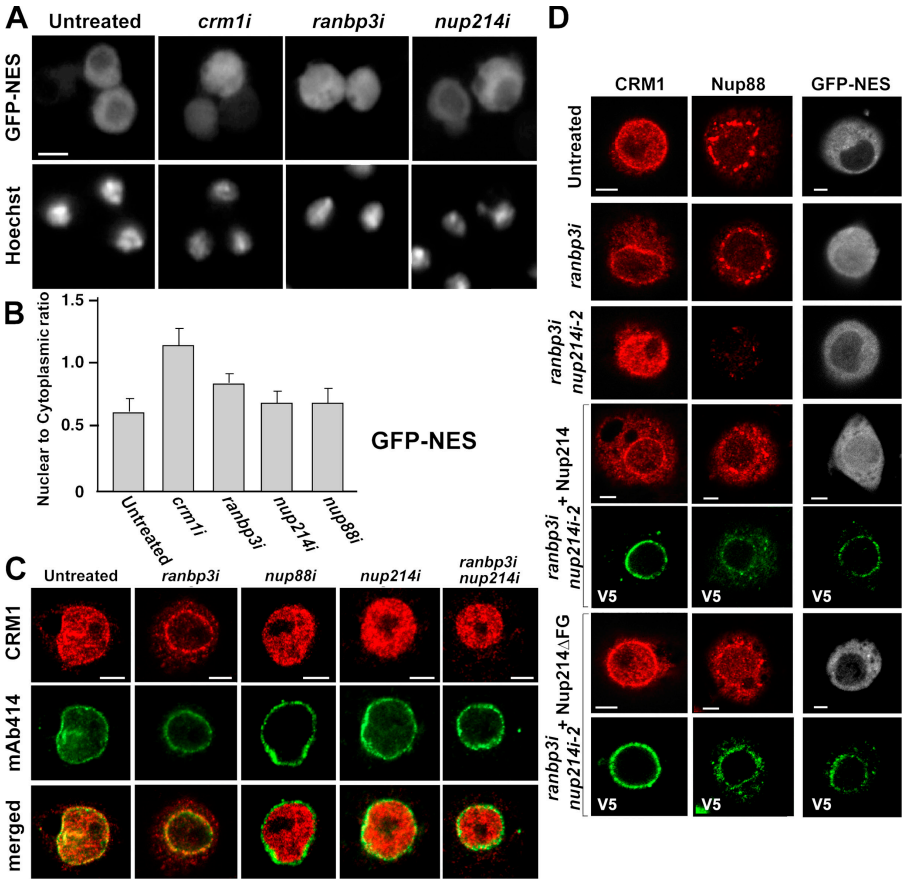


Figure 4. **Antagonistic functions of RanBP3 and Nup214 in GFP-NES export and CRM1 localization.** (A) GFP-NES–expressing cells were treated with CRM1, RanBP3, or Nup214 dsRNAs. Hoechst staining visualizes nuclei. (B) Ratios of nuclear to cytoplasmic GFP-NES in untreated cells and cells subjected to CRM1, RanBP3, Nup214, or Nup88 dsRNA treatment. CRM1 and RanBP3 RNAi cells showed the increased nuclear accumulation of GFP-NES compared with untreated cells ($P < 0.0001$ by pair-wise *t* test). Nup214 and Nup88 RNAi did not significantly alter GFP-NES distribution ($P > 0.05$ by pair-wise *t* test). Error bars indicate SD. 30–35 cells were quantified for each treatment. (C) Cells treated with RanBP3 dsRNA, Nup88 dsRNA, Nup214 dsRNA, or a combination of RanBP3 and Nup214 dsRNAs stained for CRM1 (red) and mAb414 (green). (D) Cells treated with RanBP3 dsRNA or dsRNAs against both RanBP3 and the 3′ untranslated region of Nup214 (*ranbp3i + nup214i-2*) were transfected either with V5-Nup214 or V5-Nup214ΔFG plasmids. Cells were stained for V5, Nup88, and CRM1. The right column shows GFP-NES cells treated as in other columns stained for V5 and analyzed for GFP localization. V5 staining visualizes the expression of Nup214 fusion protein. In all cases, V5 labeling is presented in green. Bars (A), 5 μm; (C and D) 2.5 μm.

expression or integrity (Fig. 3, A and B), and the cNLS-GFP mislocalization in *nup358i* cells may be caused by the massive reduction of importin β levels.

### The FG-rich region of Nup153 is required for its function in cNLS import

A common feature of Nup358, Nup153, and Nup54 is the high content of FG repeats in their primary sequence. Does the FG-rich part of Nup153 contribute to nuclear import? To address this question, we overexpressed a V5-tagged full-length (V5-Nup153) and a truncated form of Nup153 lacking the FG domain (V5-Nup153ΔFG) in Nup153 RNAi cells. Both chimeric proteins were expressed at similar levels and became localized at the nuclear envelope (Fig. 3, C and D). The full-length form restored both the pore composition defects and the cNLS-GFP phenotype (Figs. 3, C–E and S2, F–H), indicating that *Drosophila* Nup153, like its vertebrate homologues, contributes to both pore integrity and importin β transport (Walther et al., 2001). The Nup153ΔFG fragment could rescue the defects in Nup214 and TPR localization in >98% of the expressing cells ($n = 79$), suggesting that it contains all of the necessary sequences for Nup153 function in NPC integrity (Figs. 3 C and S2 H). We examined whether the Nup153ΔFG fragment is also sufficient to restore the importin β localization and cNLS import defects of Nup153 dsRNA-treated cells. In 50% of the V5-positive cells ($n = 82$), importin β accumulation resembled its steady-state localization in untreated cells (Fig. 3 C, bottom), suggesting that the Nup153 FG repeats are partly redundant for importin β localization. Restoration of the import receptor at the NPC may be caused by the reinstatement of other importin β–binding FG nucleoporins like Nup214 (Xylourgidis et al., 2006). However, only 10% of the transfected cells ($n = 66$) displayed an increased nuclear cNLS-GFP accumulation (Fig. 3, D and E). The results argue that the role of Nup153 in protein import is independent of its function in NPC integrity. The FG region is required for importin β–mediated transport, whereas the remainder of the protein ensures an intact NPC. A direct role of the Nup153-FG part in conveying importin α3/β cargos through the pore is further supported by its localization along the entire channel (Fahrenkrog et al., 2002) and by its highly flexible conformation (Lim et al., 2006).

### Antagonistic roles of Nup214 and RanBP3 in CRM1-mediated protein export

None of the dsRNA treatments against nucleoporins caused detectable defects in GFP-NES distribution (Table S1). However, the inactivation of RanBP3 increased the nuclear accumulation of the export reporter (Fig. 4, A and B). The treatment had no effect on GFP and cNLS-GFP localization (Table S1 and Fig. S3 A, available at http://www.jcb.org/cgi/content/full/jcb.200612135/DC1). Yrb2, the yeast homologue of RanBP3, is also essential for CRM1-dependent export (Taura et al., 1998; Noguchi et al., 1999). Vertebrate RanBP3 forms complexes with CRM1, RanGTP, and export substrates to stimulate NES nuclear protein export

(Englmeier et al., 2001; Lindsay et al., 2001). RanBP3 and CRM1 were also found in complex with the chromatin-associated protein RanGEF (Nemergut et al., 2002). We asked whether RanBP3 inactivation impacts CRM1 distribution by staining for CRM1. Untreated cells showed a predominantly nuclear accumulation of CRM1 with only a small fraction of the protein localized at the nuclear envelope (Figs. 4 C and S3 C). The nuclear CRM1 staining was severely reduced in RanBP3 RNAi cells. Instead, CRM1 became highly concentrated at the rim and, to some extent, in the cytoplasm of RanBP3 dsRNA-treated cells (Figs. 4 C and S3 C). The treatment had no effect on the accumulation of Nup214, Nup88, or any of the tested nucleoporins (Fig. S3 B), suggesting a new function of RanBP3 in CRM1 localization. Reexpression of V5-tagged RanBP3 at low levels in *ranBP3i* cells restored both CRM1 depletion from the nucleus and the NES export defect (Fig. S3, E and F). The results suggest that RanBP3 directly controls CRM1 localization and protein export.

CRM1 forms complexes with Nup88 and Nup214 (Fornerod et al., 1997; Roth et al., 2003), and, in *Drosophila* mutants lacking either of the nucleoporins, the NPC-bound CRM1 fraction accumulates in the nucleus (Roth et al., 2003; Xylourgidis et al., 2006). To determine whether Nup88 or Nup214 silencing causes similar phenotypes in S2 cells, we stained cells treated with Nup88 or Nup214 dsRNA for CRM1. The treatments reduced the CRM1 signal intensity at the nuclear envelope (Figs. 4 C and S3 C), suggesting that Nup88 and Nup214 anchor a CRM1 fraction at the NPC of S2 cells. However, unlike the defects of *nup88* (*mbo*) and *nup214* mutant larvae, the inactivation of Nup214 or Nup88 in S2 cells did not increase the cytoplasmic accumulation of the GFP-NES reporter (Fig. 4 A). Thus, Nup214 or Nup88 depletion has no impact on CRM1 activity in S2 cultured cells. This difference between larval tissues and S2 cells can be attributed to the relatively high levels of CRM1 bound to the NPCs of distinct larval tissues (Uv et al., 2000; Roth et al., 2003; Xylourgidis et al., 2006). The redundancy of Nup214 for NES-GFP export in S2 cells is consistent with the lack of detectable defects in the nuclear export of NLS-GFP-NES in HeLa cells depleted for Nup214 (Bernad et al., 2006). Surprisingly, RNAi inactivation of Nup214 in the same cell line resulted in defects in nuclear export of the NFAT (nuclear factor of activated T cells) transcription factor and, to a lesser extent, in export of the Rev-GR-GFP reporter (Hutten and Kehlenbach, 2006). The different phenotypes may suggest specific requirements of the different export cargoes used in the two studies.

CRM1 can shuttle between the nucleus and the cytoplasmic face of the NPC in an energy-independent manner (Becskei and Mattaj, 2003), and the inactivation of Nup214 and RanBP3 show opposing phenotypes in its localization. Therefore, we investigated CRM1 accumulation in cells treated simultaneously with both Nup214 and RanBP3 dsRNAs. In these cells, CRM1 was found inside the nucleus (Fig. 4 C), suggesting that RanBP3 and Nup214 antagonize each other to determine the nuclear concentration of CRM1. The C-terminal FG-rich region of Nup214 binds to CRM1 directly (Xylourgidis et al., 2006), and we asked whether it is also required for its antagonistic role in CRM1-mediated export. We expressed V5-tagged full-length or FG-deleted versions of Nup214 in cells lacking both RanBP3

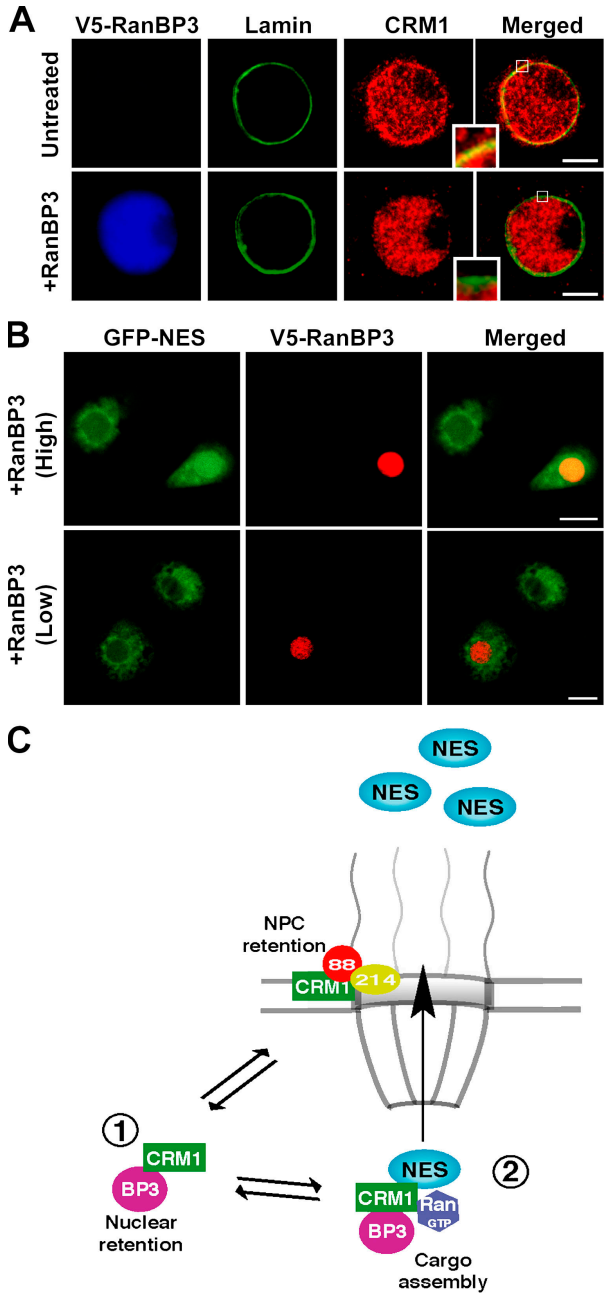


Figure 5. **RanBP3 overexpression attracts CRM1 from the NPC.** (A) Cells expressing V5-RanBP3 stained for V5 (blue), lamin (green), and CRM1 (red). Insets show magnified images of the boxed areas. (B) GFP-NES–expressing cells transfected with the V5-RanBP3 plasmid stained for V5 (red) and analyzed for the localization of GFP (green). (C) Model illustrating the postulated dynamic equilibrium between two interchangeable pools of CRM1. One is anchored by Nup214 at the NPC, and the other is retained in the nucleus by RanBP3. The model proposes two functions of RanBP3. (1) It retains CRM1 inside the nucleus. This function is antagonized by the NPC-anchoring activity of Nup214. (2) RanBP3 also promotes the assembly of NES cargo complexes and export. Bars (A), 2.5 μm; (B) 5 μm.

and Nup214, where CRM1 accumulates inside the nucleus. The V5-Nup214 protein complemented the Nup88 deficit at the nuclear envelope (Fig. 4 D, middle column) and prohibited the nuclear accumulation of CRM1 (Fig. 4 D, left column). The V5-Nup214ΔFG protein was expressed at similar levels as the wild-type protein and rescued the Nup88 degradation defect

caused by the Nup214 inactivation (Fig. 4 D; Xylourgidis et al., 2006). Thus, the N-terminal part of Nup214 is sufficient for the interaction with Nup88 and NPC. However, the V5-Nup214ΔFG fragment only slightly increased the NPC-bound fraction of CRM1 (Fig. 4 D). This small amount of CRM1 at the rim may be attracted by Nup88, which also binds to the export receptor (Roth et al., 2003). The results suggest that the antagonistic function of Nup214 on CRM1 localization is dependent on the Nup214 FG repeats.

How do the opposing roles of Nup214 and RanBP3 on CRM1 accumulation influence its activity in NES export? Treatment of GFP-NES–expressing cells with dsRNAs against both Nup214 and RanBP3 resulted in the cytoplasmic distribution of the reporter, closely resembling its accumulation in untreated cells (Fig. 4 D, right column). Thus, unleashing the pore-bound fraction of CRM1 through Nup214 inactivation largely restores the GFP-NES export defect caused by the depletion of RanBP3. The results suggest that CRM1 NES export activity can be tuned by the opposing functions of Nup214 and RanBP3. Overexpression of the full-length Nup214 construct in Nup214 and RanBP3 RNAi cells resulted in a nuclear accumulation of GFP-NES closely resembling the phenotype caused by single RanBP3 inactivation (Fig. 4 D). In contrast, the distribution of GFP-NES remained unaffected in V5-Nup214ΔFG–expressing cells lacking both Nup214 and RanBP3 (Fig. 4 D). The results indicate that the ability of Nup214 to antagonize the function of RanBP3 in NES export requires the Nup214 FG repeats.

CRM1 is reduced in the nucleus of *RanBP3i* cells, arguing that RanBP3 retains it inside the nucleus. To further examine the proposed new role of RanBP3, we overexpressed it in S2 cells and analyzed its effects on CRM1 and GFP-NES localization. The expression of V5-tagged RanBP3 increased the nuclear intensity of CRM1 (Figs. 5 A and S3 D), further arguing for a dynamic equilibrium between the Nup214- and RanBP3-bound forms of CRM1 (Fig. 5 C). In parallel experiments, we assessed the effect of RanBP3 overexpression in GFP-NES distribution. Although low levels of V5-RanBP3 did not change the predominantly cytoplasmic distribution of GFP-NES, high amounts of the exogenous protein increased the nuclear intensity of the reporter (Fig. 5 B). This phenotype is consistent with in vitro experiments in which high levels of RanBP3 inhibit the assembly of CRM1 export complexes. In summary, we propose a dual function of RanBP3 (Fig. 5 C): one maintaining high nuclear levels of CRM1 and one aiding the assembly of CRM1–RanGTP cargo complexes (Englmeier et al., 2001; Lindsay et al., 2001).

Our in vivo analysis of nucleoporin function by RNAi did not detect protein transport phenotypes for the majority of the nucleoporins. This could be the result of functional redundancy, incomplete gene inactivation, or the relatively insensitive reporter assays. Nevertheless, the data provide some new insights into the function of NPCs.

First, Nup214 and RanBP3 antagonize each other to determine CRM1 localization and function. RanBP3 has a primary role in maintaining CRM1 inside the nucleus. This function of RanBP3 becomes redundant when Nup214 is codepleted. Second, we provide genetic evidence arguing that individual FG domains are essential for distinct transport pathways in *Drosophila*. The importance of the Nup153 FG motif in mediating cNLS import was already suggested by overexpression experiments in permeabilized HeLa cells (Shah and Forbes, 1998). Surprisingly, the FG repeats of Nup214 do not facilitate NES-GFP export but rather inhibit it. The FG regions from Nup153 or Nup214 are indispensable for the distinct transport roles of Nup153 and Nup214, yet they are not expected to affect the total mass of FG repeats and the barrier function of the NPC. The genetic analysis of nucleoporins in *Drosophila* argues that the Nup153 and Nup214 FG regions have specific functions in import and export, respectively, and suggest that peripheral nucleoporins have aquired additional roles during metazoan evolution. Understanding the mechanistic roles of animal nucleoporins in endogenous protein transport may provide new insights into the regulatory potential of the NPC.

## Materials and methods

### Cell lines and cell culture

The GFP, cNLS-GFP, and GFP-NES constructs were described previously (Roth et al., 2003). S2 cells were cultured in *Drosophila* Schneider medium (PAN) supplemented with FCS, glutamine, and streptomycin/penicillin (Invitrogen). Stable cell lines were generated by hygromycin selection according to the manufacturer's instructions (Invitrogen). The expression of GFP-tagged cargoes was induced by 0.2 mM $CuSO_4$ for 16 h. Leptomycin was used at the concentration of 10 ng/ml for 15 min.

### dsRNA treatments

RNAi was performed essentially as described previously (Clemens et al., 2000). Primer pairs tailed with the T7 RNA polymerase promoter were used to amplify PCR fragments obtained from cDNA clones. PCR products with an average size of 700 bp were then used as templates for dsRNA production with the MEGAscript RNAi kit (Ambion). For transfection, 15 μg dsRNA was added to $2.5 \times 10^6$ S2 cells in six-well plates.

### Live cell imaging

DNA was visualized by the addition of Hoechst 33342 (Sigma-Aldrich) at a concentration of 4 μM. Images were recorded with an inverted fluorescence microscope (DM IRB; Leica) at days 4 and 6 after dsRNA treatment and were quantified using Volocity version 2.0.1 (Improvision).

### Western blotting and RT-PCR

Cells were lysed in 10 mM Tris, 140 mM NaCl, 1.5 mM $MgCl_2$, and 1% NP-40. Lysates were resolved by SDS-PAGE and analyzed by immunoblotting. Blots were developed using the ECL Advance kit (GE Healthcare). Images were acquired with a luminescent image analyzer (LAS1000; Fuji) and quantified with Image Gauge version 3.45 (Fuji). For RT-PCR, mRNAs were isolated using magnetic oligo(dT)-coupled beads (Dynabeads). Reverse transcription was performed with SuperScript-II (Invitrogen).

### Rescue experiments

The inactivation of Nup153 was performed with dsRNAs generated by the primers 5′-TTAATACGACTCACTATAGGGAGACATGTGTGAACAAATACCGCT-3′ and 5′-TTAATACGACTCACTATAGGGAGAGTGTGTGTGAATCTAAACGCTA-3′. Nup214 was inactivated with dsRNAs made by the primers 5′-TTAATACGACTCACTATAGGGAGATTGGTGCTGCTGCAAAGC-3′ and 5′-TTAATACGACTCACTATAGGGAGACTGAACAAGCAAAACTATTG-3′. RanBP3 was inactivated with dsRNAs generated by the primers 5′-TTAATACGACTCACTATAGGGAGACTCGCTCTTGTTCTTTTTATACG-3′ and 5′-TTAATACGACTCACTATAGGGAGAAGAGCGTGTACGATCGATATC-3′. In all cases, products were targeting the 3′ untranslated region of the respective mRNAs. The cDNA encoding full-length Nup153 (amino acids 1–1,905) and Nup153ΔFG (amino acids 1–1,288) were introduced into the BstBI site of pAc5.1/V5-His (Invitrogen). The cDNAs encoding Nup214 (amino acids 1–1,670) and Nup214ΔFG (amino acids 1–1,080) were inserted into the NotI site of pAc5.1/V5-His. The cDNA encoding RanBP3 (amino acids 1–451) was inserted into the BstBI site of pAc5.1/V5-His.

### Antibodies

We used antibodies against CRM1 (Roth et al., 2003), importin β (provided by J. Szabad, University of Szeged, Szeged, Hungary; Lippai et al., 2000),

Nup88 (Uv et al., 2000), Nup214 (Roth et al., 2003), TPR (a gift from V. Cordes, University of Heidelberg, Heidelberg, Germany), α-tubulin (Sigma-Aldrich), mAb414 (Babco), lamin (provided by G. Krohne, University of Wurzburg, Wurzberg, Germany; Wagner et al., 2004), and gp210 (provided by P.A. Fisher, Developmental Studies Hybridoma Bank, University of Iowa, Iowa City, IA; Filson et al., 1985).

**Immunofluorescence and confocal microscopy**

S2 cells were attached to poly-L-lysine– (Sigma-Aldrich) or ConA (Sigma-Aldrich)-coated coverslips. Adherent cells were fixed with 4% PFA for 30 min in PBS, permeabilized for 5 min in 0.1% Triton X-100/PBS, and incubated overnight at 4°C with primary antibodies diluted in 0.5% BSA/PBS. Cells were washed in 0.1% Triton X-100/PBS, incubated with secondary antibody for 2 h at RT, and incubated with 0.4 mg/ml DAPI for 5 min. Cells were mounted in Vectashield (Vector Laboratories). Wide-field images were acquired with Openlab version 3.1.4 (Improvision), and ratios of nuclear envelope to cytoplasmic labeling intensities were quantified using Volocity version 2.0.1 (Improvision).

Confocal images were collected with a laser-scanning microscope (LSM510; Carl Zeiss MicroImaging, Inc.) and processed with LSM510 software (Carl Zeiss MicroImaging, Inc.). For quantitative analysis of confocal images, the nuclear membrane was reduced to a binary image. A distance transform function was applied, producing separate maps of distances into the nucleus and the cytoplasm. The distance maps were used to define regions of interest at increasing distances from the nuclear membrane. The nucleolus, areas outside the cell, vacuoles, and nuclear membrane folds were excluded from the analysis. The average concentration gradient for a cell population was obtained by giving equal weight to the individual concentration gradients. Software was based on a Semper6w kernel (Syncroscopy).

**Online supplemental material**

Table S1 summarizes the transport phenotypes after dsRNA treatment against *Drosophila* nucleoporins. Fig. S1 shows importin α/β and CRM1 transport assays in *Drosophila* S2 cells (A and B) and shows the inactivation efficiency in dsRNA-treated cells (C–E). Fig. S2 shows the cNLS-GFP import defect in cells treated with the second set of Nup358, Nup153, and Nup54 dRNAs (A–C) and shows CRM1 and GFP-NES localization in cells defective in cNLS-GFP import (D and E). Fig. S2 also shows the restoration of TPR and Nup214 localization by full-length Nup153 or Nup153ΔFG (F–H). Fig. S3 shows the NPC integrity and cNLS-GFP import in RanBP3 RNAi cells (A and B) and shows that Nup214 and RanBP3 determine the CRM1 concentration at the pore (C and D). Fig S3 also shows the restoration of CRM1 localization and protein export activity in RanBP3 RNAi cells (E and F). Online supplemental material is available at http://www.jcb.org/cgi/content/full/jcb.200612135/DC1.

We are indebted to V. Cordes, J. Szabad, G. Krohne, and the Developmental Studies Hybridoma Bank for antibodies. We thank K. Senti, L. Wieslander, S. Gee, and M. Mannervik for constructive comments.

This work was supported by grants from VetenskapsRadet, Cancerfonden, and Wallenberg Consortium North to C. Samakovlis. F. Sadeghifar was supported by a scholarship from the Iranian Ministry of Science, Research, and Technology.

Submitted: 22 December 2006
Accepted: 11 July 2007

## References

Bayliss, R., T. Littlewood, L.A. Strawn, S.R. Wente, and M. Stewart. 2002. GLFG and FxFG nucleoporins bind to overlapping sites on importin-beta. *J. Biol. Chem.* 277:50597–50606.

Becskei, A., and I.W. Mattaj. 2003. The strategy for coupling the RanGTP gradient to nuclear protein export. *Proc. Natl. Acad. Sci. USA*. 100:1717–1722.

Bernad, R., D. Engelsma, H. Sanderson, H. Pickersgill, and M. Fornerod. 2006. Nup214-Nup88 nucleoporin subcomplex is required for CRM1-mediated 60 S preribosomal nuclear export. *J. Biol. Chem.* 281:19378–19386.

Bucci, M., and S.R. Wente. 1998. A novel fluorescence-based genetic strategy identifies mutants of *Saccharomyces cerevisiae* defective for nuclear pore complex assembly. *Mol. Biol. Cell*. 9:2439–2461.

Clemens, J.C., C.A. Worby, N. Simonson-Leff, M. Muda, T. Maehama, B.A. Hemmings, and J.E. Dixon. 2000. Use of double-stranded RNA interference in *Drosophila* cell lines to dissect signal transduction pathways. *Proc. Natl. Acad. Sci. USA*. 97:6499–6503.

Collier, S., H.Y. Chan, T. Toda, C. McKimmie, G. Johnson, P.N. Adler, C. O'Kane, and M. Ashburner. 2000. The *Drosophila* embargoed gene is required for larval progression and encodes the functional homolog of *Schizosaccharomyces* Crm1. *Genetics*. 155:1799–1807.

Cordes, V.C., S. Reidenbach, H.R. Rackwitz, and W.W. Franke. 1997. Identification of protein p270/Tpr as a constitutive component of the nuclear pore complex-attached intranuclear filaments. *J. Cell Biol.* 136:515–529.

Cronshaw, J.M., A.N. Krutchinsky, W. Zhang, B.T. Chait, and M.J. Matunis. 2002. Proteomic analysis of the mammalian nuclear pore complex. *J. Cell Biol.* 158:915–927.

Englmeier, L., M. Fornerod, F.R. Bischoff, C. Petosa, I.W. Mattaj, and U. Kutay. 2001. RanBP3 influences interactions between CRM1 and its nuclear protein export substrates. *EMBO Rep.* 2:926–932.

Fahrenkrog, B., B. Maco, A.M. Fager, J. Koser, U. Sauder, K.S. Ullman, and U. Aebi. 2002. Domain-specific antibodies reveal multiple-site topology of Nup153 within the nuclear pore complex. *J. Struct. Biol.* 140:254–267.

Filson, A.J., A. Lewis, G. Blobel, and P.A. Fisher. 1985. Monoclonal antibodies prepared against the major *Drosophila* nuclear Matrix-pore complex-lamina glycoprotein bind specifically to the nuclear envelope in situ. *J. Biol. Chem.* 260:3164–3172.

Finlay, D.R., E. Meier, P. Bradley, J. Horecka, and D.J. Forbes. 1991. A complex of nuclear pore proteins required for pore function. *J. Cell Biol.* 114:169–183.

Fornerod, M., J. van Deursen, S. van Baal, A. Reynolds, D. Davis, K.G. Murti, J. Fransen, and G. Grosveld. 1997. The human homologue of yeast CRM1 is in a dynamic subcomplex with CAN/Nup214 and a novel nuclear pore component Nup88. *EMBO J.* 16:807–816.

Frey, S., R.P. Richter, and D. Gorlich. 2006. FG-rich repeats of nuclear pore proteins form a three-dimensional meshwork with hydrogel-like properties. *Science*. 314:815–817.

Hutten, S., and R.H. Kehlenbach. 2006. Nup214 is required for CRM1-dependent nuclear protein export in vivo. *Mol. Cell. Biol.* 26:6772–6785.

Lim, R.Y., N.P. Huang, J. Koser, J. Deng, K.H. Lau, K. Schwarz-Herion, B. Fahrenkrog, and U. Aebi. 2006. Flexible phenylalanine-glycine nucleoporins as entropic barriers to nucleocytoplasmic transport. *Proc. Natl. Acad. Sci. USA*. 103:9512–9517.

Lindsay, M.E., J.M. Holaska, K. Welch, B.M. Paschal, and I.G. Macara. 2001. Ran-binding protein 3 is a cofactor for Crm1-mediated nuclear protein export. *J. Cell Biol.* 153:1391–1402.

Lippai, M., L. Tirian, I. Boros, J. Mihaly, M. Erdelyi, I. Belecz, E. Mathe, J. Posfai, A. Nagy, A. Udvardy, et al. 2000. The Ketel gene encodes a *Drosophila* homologue of importin-beta. *Genetics*. 156:1889–1900.

Malik, H.S., T.H. Eickbush, and D.S. Goldfarb. 1997. Evolutionary specialization of the nuclear targeting apparatus. *Proc. Natl. Acad. Sci. USA*. 94:13738–13742.

Nemergut, M.E., M.E. Lindsay, A.M. Brownawell, and I.G. Macara. 2002. Ran-binding protein 3 links Crm1 to the Ran guanine nucleotide exchange factor. *J. Biol. Chem.* 277:17385–17388.

Noguchi, E., Y. Saitoh, S. Sazer, and T. Nishimoto. 1999. Disruption of the YRB2 gene retards nuclear protein export, causing a profound mitotic delay, and can be rescued by overexpression of XPO1/CRM1. *J. Biochem. (Tokyo)*. 125:574–585.

O'Brien, K.P., M. Remm, and E.L. Sonnhammer. 2005. Inparanoid: a comprehensive database of eukaryotic orthologs. *Nucleic Acids Res.* 33:D476–D480.

Roth, P., N. Xylourgidis, N. Sabri, A. Uv, M. Fornerod, and C. Samakovlis. 2003. The *Drosophila* nucleoporin DNup88 localizes DNup214 and CRM1 on the nuclear envelope and attenuates NES-mediated nuclear export. *J. Cell Biol.* 163:701–706.

Rout, M.P., J.D. Aitchison, A. Suprapto, K. Hjertaas, Y. Zhao, and B.T. Chait. 2000. The yeast nuclear pore complex: composition, architecture, and transport mechanism. *J. Cell Biol.* 148:635–651.

Rout, M.P., J.D. Aitchison, M.O. Magnasco, and B.T. Chait. 2003. Virtual gating and nuclear transport: the hole picture. *Trends Cell Biol.* 13:622–628.

Shah, S., and D.J. Forbes. 1998. Separate nuclear import pathways converge on the nucleoporin Nup153 and can be dissected with dominant-negative inhibitors. *Curr. Biol.* 8:1376–1386.

Strawn, L.A., T. Shen, N. Shulga, D.S. Goldfarb, and S.R. Wente. 2004. Minimal nuclear pore complexes define FG repeat domains essential for transport. *Nat. Cell Biol.* 6:197–206.

Taura, T., H. Krebber, and P.A. Silver. 1998. A member of the Ran-binding protein family, Yrb2p, is involved in nuclear protein export. *Proc. Natl. Acad. Sci. USA*. 95:7427–7432.

Tran, E.J., and S.R. Wente. 2006. Dynamic nuclear pore complex: life on the edge. *Cell*. 125:1041–1053.

Uv, A.E., P. Roth, N. Xylourgidis, A. Wickberg, R. Cantera, and C. Samakovlis. 2000. members only encodes a *Drosophila* nucleoporin required for rel protein import and immune response activation. *Genes Dev.* 14:1945–1957.

Wagner, N., J. Schmitt, and G. Krohne. 2004. Two novel LEM-domain proteins are splice products of the annotated *Drosophila* melanogaster gene CG9424 (Bocksbeutel). *Eur. J. Cell Biol.* 82:605–616.

Walther, T.C., M. Fornerod, H. Pickersgill, M. Goldberg, T.D. Allen, and I.W. Mattaj. 2001. The nucleoporin Nup153 is required for nuclear pore basket formation, nuclear pore complex anchoring and import of a subset of nuclear proteins. *EMBO J.* 20:5703–5714.

Walther, T.C., H.S. Pickersgill, V.C. Cordes, M.W. Goldberg, T.D. Allen, I.W. Mattaj, and M. Fornerod. 2002. The cytoplasmic filaments of the nuclear pore complex are dispensable for selective nuclear protein import. *J. Cell Biol.* 158:63–77.

Wozniak, R.W., and G. Blobel. 1992. The single transmembrane segment of gp210 is sufficient for sorting to the pore membrane domain of the nuclear envelope. *J. Cell Biol.* 119:1441–1449.

Xylourgidis, N., P. Roth, N. Sabri, V. Tsarouhas, and C. Samakovlis. 2006. The nucleoporin Nup214 sequesters CRM1 at the nuclear rim and modulates NFkappaB activation in *Drosophila*. *J. Cell Sci.* 119:4409–4419.